SHocks: structure, AcceleRation, dissiPation

Work Package 4
Exploring acceleration in astrophysical shocks through broadband emission

Deliverable D4.3
Technical report on the analysis of IXPE observations of Cassiopeia A

Jacco Vink & Dmitry Prokhorov

Anton Pannekoek Institute & GRAPPA, University of Amsterdam, Science Park 904, 1098 XH Amsterdam, The Netherlands

28/10/2022

This project has received funding from the European Union's Horizon 2020 research and innovation programme under grant agreement No 101004131

Document Change Record

Issue	Date	Author	Details
1	28/10/2022	J. Vink & D. Prokhorov	

Table of Contents

1 Summary

In this technical report we report on the analysis of the data obtained by the NASA/ASA The Imaging X-ray Polarimetry Explorer (IXPE) mission. IXPE was launched on December 9, 2022, and its first science target was the supernova remnant (SNR) Cassiopeia A (Cas A). Cas A is a ∼350 yr old SNR, and one of a handful of young SNRs known to emit synchrotron radiation in X-rays from regions close to the actively accelerating shock fronts. Synchrotron radiation is intrinsically linearly polarized, with polarization fractions of more than 70%. The polarization vector of synchrotron radiation is perpendicular to the magnetic field direction. However, the presence of turbulent magnetic fields along the line of sight reduce the polarization fraction. Polarimetric measurement s, therefore, inform us about the level of magnetic-field turbulence. The IXPE analysis of observations of Cas A indicates a very low polarization fraction ($\lesssim 5\%$), and a radially oriented magnetic field. The low polarization fraction indicates a high level of magnetic-field turbulence behind the shock fronts of Cas A. The radial orientation is in line with earlier radio polarization measurements, but in X-rays they pertain to the magnetic fields much closer to the shock fronts. At the shock fronts one expects a predominantly tangential magnetic-field orientation due to the compression of a, likely isotropic, magnetic field upstream of the shock.

2 Introduction

The collisionless shocks of SNRs are thought to be the dominant sites of cosmic-ray acceleration in the Milk Way. The main reason for this that only supernovae provide enough power to maintain the energy density in cosmic rays in the galaxy [Chapter 11 in Vink, 2020, summarizes the arguments]. A central piece of evidence that indeed SNR are active sites of cosmic-ray acceleration is formed by the detection of X-ray synchrotron radiation by relativistic electrons from near the shock regions in young SNRs. Although the electron cosmic rays make up only a small fraction of cosmic rays, their radiative properties are revealing the acceleration process.

The X-ray synchrotron radiation is caused by relativistic electrons with energies $\gtrsim 10$ TeV. Energetic electrons lose their energy quickly, within a time scale $\tau_{\rm loss} \approx 12.5(B/100\ \mu{\rm G})^{-2}(E/10^{14}\ eV)$ yr, implying loss time scales of 5–20 yr for the downstream magnetic-field strength in Cas A of $\sim 250\ \mu$G [e.g. Helder et al., 2012]. The X-ray synchrotron emitting regions in Cas A are located at the forward shock around the whole SNR, but also near the reverse shock regions, in particular in the western part. The implications are that Cas A actively accelerates electrons up to $\sim$ 10 TeV, in a time scale fast than the 5–20 yr loss time scale. The acceleration mechanism is generally accepted to be diffusive shock acceleration [DSA, e.g. Bell, 1978, Malkov and Drury, 2001], which operates by having energetic particles diffusively cross the shock front repeatedly. Since the loss time scale for electrons is so short, X-ray synchrotron radiation requires fast acceleration to the 10 TeV regime, which according to DSA requires turbulent and relatively strong magnetic fields in the 100–500 μG range.

The magnetic-field turbulence is thought to be self-generated by the cosmic rays upstream of the shock, i.e. in the cosmic-ray shock precursor. The generation of turbulence is either resonant turbulence, i.e. charged particles with gyroradii $r_g(E)$ generate Alfvén waves with wavelength of $\lambda_B \approx r_g$, or non-resonant waves, which can have typical length scale. For the non-resonant case most focus has been on the Bell-instability [Bell, 2004], which is caused by the return current in the upstream medium, associated with a net current caused by the streaming of cosmic rays.

X-ray synchrotron radiation of young SNRs was first revealed in 1995 for SN1006 [Koyama et al., 1995] and now we know that all young SNRs with fast shocks ($V_s \gtrsim 3000\,\mathrm{km\,s^{-1}}$) display X-ray synchrotron emission. The ultimate proof that we are indeed detecting synchrotron emission is to detect X-ray polarization. Moreover, polarization signals provide us with information on the magnetic-field turbulence properties, an important ingredient of DSA, and the magnetic-field orientation.

The latter point is important. Radio synchrotron radiation shows that young SNRs have radially oriented magnetic-fields, whereas older SNRs have tangentially oriented magnetic-field directions [e.g. Dubner and Giacani, 2015, for a review]. There is natural explanation for tangential magnetic fields: if an upstream turbulent field is shock compressed, the tangential component will be enhanced. Why this is not happening for young SNRs is not clear. Possible explanations long focussed on Rayleigh-Taylor instabilities in the plasma [Jun and Norman, 1996], but this operates mostly in the interior, not near the shock. However, there may be instabilities at the shock as well [Inoue et al., 2013]. A question is, therefore, whether the radial magnetic-field is already present near the shock.

X-ray synchrotron emission from the young SNR Cas A comes from within $1''$–$2''$ of the shock front, much narrower than the radio synchrotron radiation, which comes from the entire shell. Cas A was the first science target of the NASA/ASI small explorer mission Imaging X-ray Polarimetry Explorer (IXPE), launched on December 9, 2021. The first results were recently published [Vink et al., 2022b], and here a summary is given. The preprint is added to the this technical report.

3 IXPE observations of Cas A

IXPE is a small satellite mission [Weisskopf et al., 2022], and consists of a spacecraft with three nested X-ray mirrors, located at the end of an extendable boom, and three detector units in the focal planes of the mirrors. The detector units use gas-pixel-detectors (GPDs) filled with dimethyl ether [Costa et al., 2001, Baldini et al., 2021]. An X-ray photon interacting with the gas will liberate photo-electron, whose direction will be correlated with the electric field of the X-ray photon, with a proportionality $\phi \propto \cos^2\theta$, with θ the electric field direction and ϕ the photo-electron's direction. The photo-electron causes further ionizations, resulting in an electron cloud, whose overall shape reflects ϕ. An ASIC at the bottom of the detector reads out the electron cloud, and the data are stored and send to Earth for estimating ϕ and the energy of the photon event.

The spatial resolution of IXPE is $\sim 25''$, which means that the X-ray synchrotron filaments cannot be resolved.

Cas A was observed by IXPE in January 2022 for about 1 Ms. The data were analyzed within the IXPE supernova remnants working group (WG), chaired by

Dr Pat Slane (CfA), and the particular effort on Cas A was led by Dr J. Vink in close collaboration with several other WG members, including SHARP member D. Prokhorov, who was responsible for generating Stokes I, Q, and U maps, as well as performing simulations in order to disentangle the thermal and synchrotron radiation components. For the latter an input spectral map was made by J. Vink based on Chandra X-ray observations, details of which can be found in the appendix of the publication, as well as Zenodo (doi:10.5281/zenodo.6597504).

Since the data analysis concerned the first science data taken by IXPE and this was done shortly after launch, several unexpected hurdles had to be taken. One of them was that the telescopes were not fully aligned, and the coordinates contained errors. These had to be corrected, using a procedure described in Vink et al. [2022a].

4 Results

For the analysis we used events with reconstructed photon energies in the 3–6 keV range. IXPE's polarization sensititivity peaks in this range, and it includes the nearly line emission free band of 4–6 keV, while at the same time avoiding the 1.7–2.5 keV range in which the Cas A spectrum is dominated by line emission from silicon and sulphur.

The initial analysis focussed on the imaging analysis, i.e. maps were made in the Stokes I, Q, and U parameters. The software *ixpesobsim* also produced the variance maps of these parameters, and we made use of the fact that Q and U are independent quantities, so we can use χ^2 statistics:

$$\chi^2_2 = \frac{Q^2_{i,j}}{\mathrm{Var}(Q_{i,j})} + \frac{U^2_{i,j}}{\mathrm{Var}(U_{i,j})}, \tag{1}$$

with the subscripts i, j indicating that this is a statistic for each pixel.

The Stokes I map (just an intensity map) is shown in Fig. 1, and examples of the Stokes Q and U maps are shown in Fig. 2. These maps do show high significance detections of polarization (at the 3σ) level. However, the IXPE map of Cas A has about 200 resolution elements, and maps with different pixel size have been analyzed. Under these circumstance 3σ is too low in confidence: on average we expect about 1 or 2 pixels with spurious detections. The maps do, however, show that the polarization fraction must be low, $\lesssim 12\%$ at the periphery of Cas A and less than 5% in the interior.

We also experimented with smoothed maps (not in the official publication), which shows even lower polarization fractions, and consistent regions of relatively high polarization.

However, a confident polarization detection was made using a special procedure: we expect the net magnetic-field structure to be either radially oriented (based on previous radio maps), or tangentially oriented, as this is expected from shock compression. If we sum regular Stokes Q and U parameters over large region this would result in a low polarization in these cases. But by redefining the orientation of Q and U depending on the polar coordinates within Cas A, i.e. enforcing circular symmetry, we can coherently add up the Stokes Q and U parameters over large parts of Cas A.

The summations were done for the regions indicated in Fig. 1. A priori we expect the strongest signals to be at the outskirts, where the synchrotron filaments associated with the forward shock are located, or in the western part, where synchrotron radiation associated with (parts of) the reverse shock is located [see also Vink et al., 2022a]. The measured polarization degree and direction are visualized in Fig. 3. It shows that significant polarization is detected in the forward shock region, and even more significantly so if the western reverse shock region is added. The polarization fraction is low $\leq 3\%$ before correcting for thermal components, and $\leq 4.5\%$ after correction for thermal radiation, i.e. for the synchrotron component only.

Surprisingly the net magnetic-field direction is radial, even though the X-ray synchrotron radiation is coming from within a narrow ($\lesssim 10^{17}$ cm, 1–2″) region of the shock front.

The main conclusions are: 1) the magnetic-field downstream of the shocks is likely highly turbulent, despite the fact that the shock compression must have initially created an overall tangential magnetic field; 2) the radial magnetic-field is established relatively close to the shock front. Conclusion 1) is a surprising as theoretical papers rarely discuss the possibility of very turbulent (isotropic) magnetic fields downstream of the shock. However, we have to point out that also a near 50%/50% mix of tangential and radial magnetic-field topology can result in a low polarization fraction.

5 Discussion in the context of collissionless shocks

Within the framework of SHARP project, it is interesting to discuss the IXPE results in the context of collisionless shocks in general. Much of the SHARP project is devoted in situ measurements of collisionless shocks. The downstream length scales over which properties are measured in situ are of the order of 10^7 cm, as compared to the 10^{17} cm (Chandra resolution) to 10^{18} cm (IXPE resolution) discussed in this report.

Nevertheless, it is of interest to investigate the occurrence of magnetic-field turbulence near the shock, the preferred magnetic-field directions imposed, and how these conditions change immediately downstream of the shock, at the 10^7 cm as measured in situ in space plasmas. Is there already evidence for a preferred magnetic-field direction, or reorientation, at these small scales. And how do these depend on Mach numbers?

The IXPE results make it clear that the magnetic-field reorientation must happen in the shock region. It could be caused by hydrodynamical instabilities. One possibility is that the seeds for these instabilities may be the rippling of shocks as discussed in Deliverable D2.2. As it is observationally difficult to connect the in situ observations with the IXPE results, future work may concentrate on the theoretical implication, either analytically or numerically.

6 References

L. Baldini et al. Design, construction, and test of the Gas Pixel Detectors for the IXPE mission. *Astroparticle Physics*, 133:102628, December 2021.

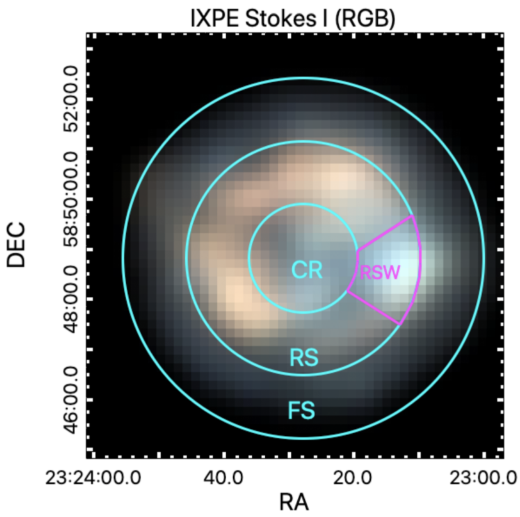

Figure 1: Left: IXPE three color Stokes I image with square-root brightness scaling, based on the 2–3 keV, 3–4 keV, and 4–6 keV bands, combined from the three detectors. The pixel size is $10.4''$ and the images have been smoothed with a gaussian kernel with $\sigma = 10.4''$. The regions indicated correspond to the summed analyses.

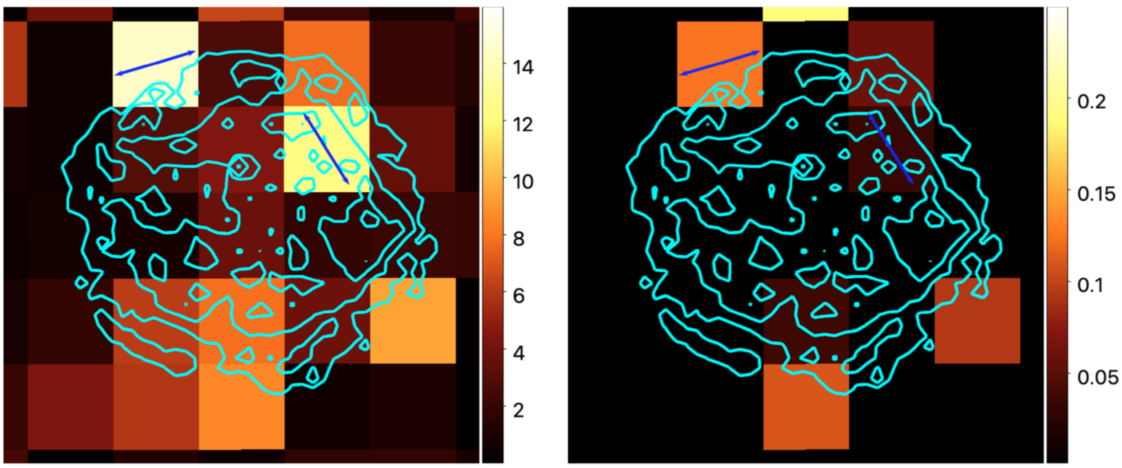

Figure 2: Maps reproduced from Vink et al. [2022b]. Left: Maps of χ_2^2 (or $S_{i,j}$ values for the polarization signal for the 3-6 keV band. The pixel size is $84''$. Right: the corresponding polarization degree maps. Only pixels with pre-trial confidence levels above 2σ ($\chi_2^2 > 6.28$) are shown. Peaks in the χ_2^2 map are $\chi_2^2 = 14.4, 12.3$ corresponding to polarization degrees of 12.4% and 3.4%.

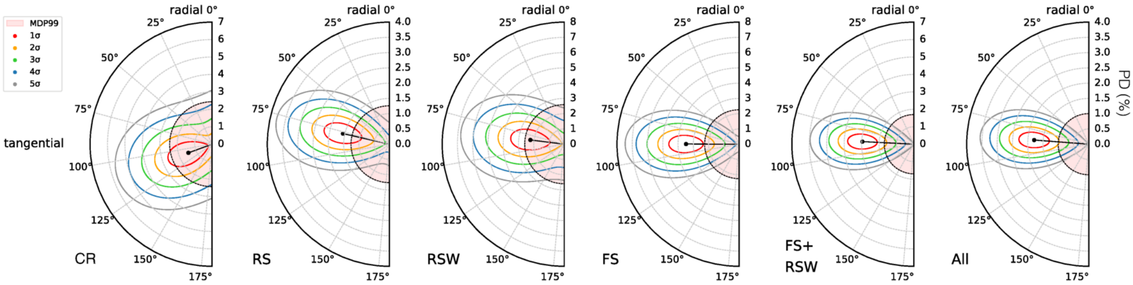

Figure 3: Reproduced from Vink et al. [2022b]. Polar diagrams depicting the measured polarization degree and angle with respect to circular symmetry as confidence contours for six regions. The radial coordinate indicates the polarization degree in percent. The pink region corresponds to the MDP99 level. Values around 90° correspond to an overal tangentially oriented polarization averaged over the region, while around 0° indicates on average a radially oriented polarization.

DOI:10.1016/j.astropartphys.2021.102628.

A. R. Bell. The acceleration of cosmic rays in shock fronts. I. *MNRAS*, 182:147–156, January 1978. URL http://adsabs.harvard.edu/cgi-bin/nph-bib_query?bibcode=1978MNRAS.182..147B&db_key=AST.

A. R. Bell. Turbulent amplification of magnetic field and diffusive shock acceleration of cosmic rays. *MNRAS*, 353:550–558, September 2004.

E. Costa, P. Soffitta, R. Bellazzini, A. Brez, N. Lumb, and G. Spandre. An efficient photoelectric X-ray polarimeter for the study of black holes and neutron stars. *Nat*, 411:662–665, June 2001.

G. Dubner and E. Giacani. Radio emission from supernova remnants. *A&A Rev.*, 23:3, September 2015. DOI:10.1007/s00159-015-0083-5.

E. A. Helder, J. Vink, A. M. Bykov, Y. Ohira, J. C. Raymond, and R. Terrier. Observational Signatures of Particle Acceleration in Supernova Remnants. *SSRv*, 173:369–431, November 2012. DOI:10.1007/s11214-012-9919-8.

Tsuyoshi Inoue, Jiro Shimoda, Yutaka Ohira, and Ryo Yamazaki. The Origin of Radially Aligned Magnetic Fields in Young Supernova Remnants. *ApJ*, 772(2): L20, August 2013. DOI:10.1088/2041-8205/772/2/L20.

B.-I. Jun and M. L. Norman. On the Origin of Radial Magnetic Fields in Young Supernova Remnants. *ApJ*, 472:245–+, November 1996. DOI:10.1086/178059.

K. Koyama et al. Evidence for Shock Acceleration of High-Energy Electrons in the Supernova Remnant SN 1006. *Nat*, 378:255–+, November 1995.

M. A. Malkov and L. Drury. Nonlinear theory of diffusive acceleration of particles by shock waves . *Reports of Progress in Physics*, 64:429–481, April 2001.

J. Vink. *Physics and Evolution of Supernova Remnants*. Astronomy and Astrophysics Library. Springer International Publishing, 2020. ISBN 9783030552299. URL https://books.google.nl/books?id=WgSYzQEACAAJ.

Jacco Vink, Daniel J. Patnaude, and Daniel Castro. The Forward and Reverse Shock Dynamics of Cassiopeia A. *ApJ*, 929(1):57, April 2022a. DOI:10.3847/1538-4357/ac590f.

Jacco Vink, Dmitry Prokhorov, Riccardo Ferrazzoli, Patrick Slane, Ping Zhou, et al. X-Ray Polarization Detection of Cassiopeia A with IXPE. *ApJ*, 938(1): 40, October 2022b. DOI:10.3847/1538-4357/ac8b7b.

M.C. Weisskopf, P. Soffitta, L. Baldini, et al. Imaging X-ray Polarimetry Explorer: prelaunch. *Journal of Astronomical Telescopes, Instruments, and Systems*, 8(2): 1 – 28, 2022. DOI:10.1117/1.JATIS.8.2.026002. URL `https://doi.org/10.1117/1.JATIS.8.2.026002`.